http://dx.doi.org/10.5012/bkcs.2014.35.4.1218

Preparation of Exfoliated Ag-Laponite Nanocomposites Through a Freeze-Drying of Laponite Sols

Seung-Kyu Yang, Jeong-Won Nam, and Youhyuk Kim*

Department of Chemistry, College of Natural Sciences, Dankook University, Cheonan, Chungnam 330-714, Korea
**E-mail: hyukim@dankook.ac.kr*
Received December 10, 2013, Accepted December 29, 2013

Key Words : Colloidal processing, Exfoliation, Nanocomposites, X-ray techniques, Thermal properties

Colloidal Ag and Au nanoparticles have been intensively studied due to their potential and real applications varying from optics and catalysis to biomedicine.[1-3] Many methods exist for the synthesis of Ag and Au nanoparticles, but most processes result in low nanoparticle concentrations due to aggregation into large particles.[4,5] Surfactants, thiols or clays as capping agents or stabilizing reagents have been used effectively to prevent the growth and aggregation of nanoparticles. In particular, high concentrations of Ag colloidal sol have been obtained using synthetic layered clay, laponite as a steric barrier to prevent aggregation of Ag nanoparticles.[6]

The use of clay for high concentrations of noble metal nanoparticles generates nanoparticle/clay composites that are believed to be important materials with a large variety of applications in functionalized ceramics, adsorbents, ion exchanger and catalysts.[7] Noble metal nanoparticles in layered clays are distributed into central layer spaces and/or on the external surfaces. The adsorption of Ag nanoparticles on the external surfaces and edges of talc in Ag-talc nanocomposites were suggested based on X-ray diffraction results that showed little variation of basal d_{001}-spacing.[8] In the case of kaolinite and montmorillonite, intercallation of small Ag nanoparticles or Ag clusters in the interlamellar space of layered clay minerals was reported, as well as the formation of larger Ag nanoparticles on the exterior surface of these clays.[9-12] However, exfoliated noble metal-clay nanocomposites are rare in spite of expected high performance due to large surface areas of clays to allow interactions with nanometals.

We have been interested in a colloidal synthesis procedure and found a simple method for very stable (> 24 months) Ag nanoparticle sols with laponite. The natural hectorite of the smectites, laponite is utilized as a stabilizing reagent in this synthesis and forms the basis for production of highly concentrated solutions of Ag nanoparticles. Laponite is a synthetic polycrystalline clay and the empirical composition is $Na_{0.7}[(Si_8Mg_{5.5}Li_{0.3})O_{20}(OH)_4]$.[6] The structure of laponite consists of layers formed by the condensation of two outer layers of linked $Si(O,OH)_4$ tetrahedra with a central layer of linked $M(OH)_6$ octahedra, where M is either an Mg or Li ion. Part of the magnesium ions in the central layer are substituted by lithium ions, resulting in a net negative charge of the layer, which is balanced by sodium ions located between adjacent layers in a stack. The sodium ions in laponite are exchangeable, and in aqueous dispersions, these ions diffuse into the water, and plate-like particles with negatively charged faces are formed. This work reports on Ag nanoparticles-laponite composites prepared by a freeze-drying method from resulting Ag nanoparticle sols. The adsorption behavior of Ag nanoparticles into laponite is investigated.

As the concentration of $AgNO_3$ increased, the intensity of the absorption peak at about 397~407 nm in UV-vis spectra of Ag colloids increased, as shown in Figure 1. The absorption peak at about 400 nm in Figure 1 is characteristic of surface plasmon resonance absorption of Ag nanoparticles.[13] With the increase of silver nitrate concentration, absorption peaks at about 405 nm slightly shifted to the shorter wavelength of about 5-8 nm and new bands at about 418 and 545 nm appeared, as shown in Figure 1(c) and (d). It is reasonable that absorption peaks at the shorter wavelength are assigned to small silver nanoparticles adsorbed on laponite and new bands at a longer wavelength are associated with the aggregation of Ag nanoparticles growing into larger particles with increasing silver content in aqueous solution. Figure 2 shows the result of TEM observation in which small particles prevailed at low concentrations (Figure 2(a), (b)) and above this concentration silver nanoparticles were

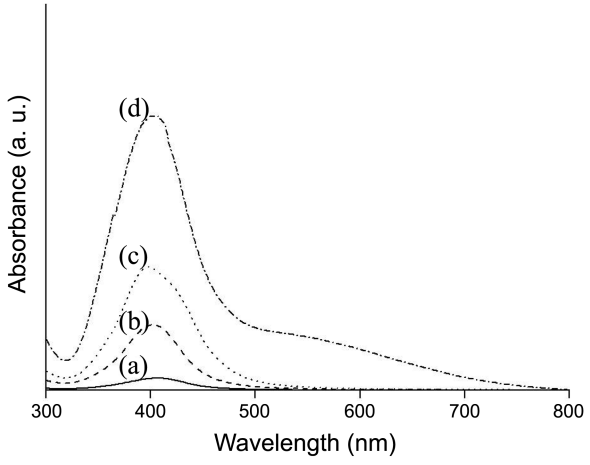

Figure 1. UV-vis absorption spectra of silver colloids as a function of $AgNO_3$ concentrations: (a) 0.05, (b) 0.25, (c) 0.50, (d) 2.5 mmol.

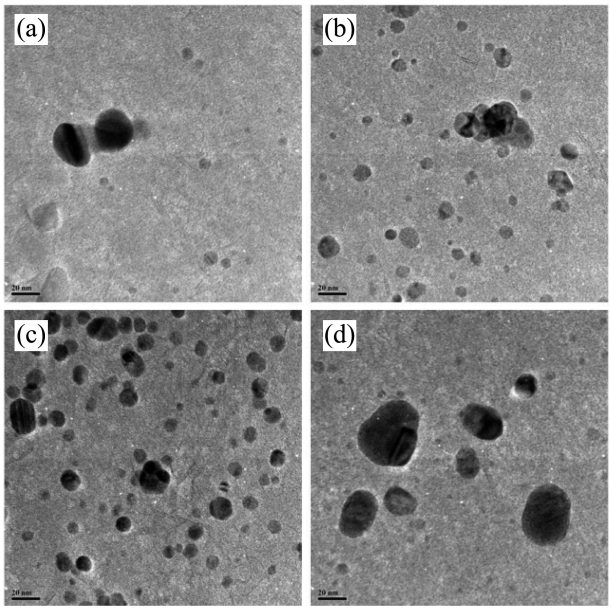

Figure 2. TEM micrographs of nanosilver particles prepared in various concentrations of $AgNO_3$: (a) 0.05, (b) 0.25, (c) 0.50, (d) 2.5 mmol. The scale bar represents 20 nm.

aggregated and larger particles were formed (Figure 2(c) and (d)). These TEM results are consistent with those of UV-vis. The particle sizes of small particles and larger particles in Figure 2(c) are about 3-8 nm and about 10-20 nm, respectively. Figure 3 shows X-ray patterns of Ag nanoparticles-laponite composites, in which the Ag nanoparticles revealed X-ray patterns characteristic of silver, although the degree of crystallinity was different. While the peaks for Ag nanoparticles are broad when the silver content is low, they sharpen when the amount of silver present is high. The size of Ag nanoparticles using the Scherrer Formula[14] was calculated from the (111) reflection in the XRD patterns. The nanosilver particle diameter increases with the increase in the silver content, as shown in Figure 3. These XRD results reveal that sizes of Ag nanoparticles are in the range of 7.5-20.3 nm and this agrees with those of TEM, as shown in Figure 2. The XRD patterns of Ag-laponite nanocomposites in Figure 3(a)-(c) show broad peaks with basal d_{001} spacings of about 1.40 to 1.47 nm calculated from the d_{001} reflection at about $2\theta = 6.80^0$, corresponding to an interlayer distances of about 0.44 to 0.51 nm. The interlayer distance is obtained after subtracting the thickness of the intrinsic silicate layer (~0.96 nm) from the basal spacing.[15] The sharpness of the d_{001} reflection in Figures 3(a)-(c) suggests that the layers of laponite during freeze-drying are stacked face to face in ordered tactoids. The intercalation of Ag nanoparticles into the interlayer of laponite is excluded, because the particle sizes obtained from the TEM micrographs in Figure 2 and XRD data in Figure 3 are too large to be accommodated between the layers of the clay. A considerable amount of nanosilver particles are to be deposited on the external surfaces of the clay. With high nanosilver concentrations, most of the d_{001} reflections and peaks characteristic of

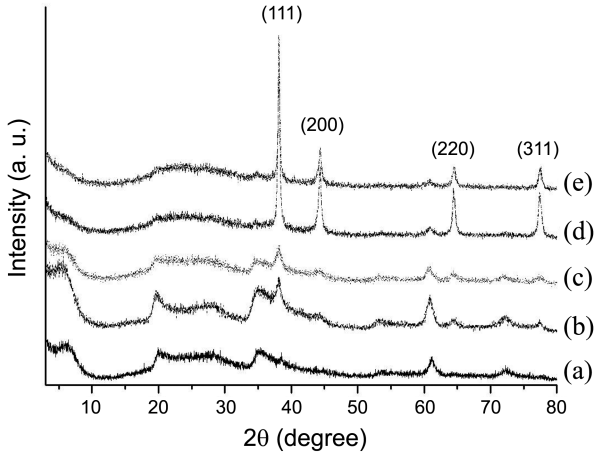

Figure 3. XRD patterns of Ag-laponite nanocomposites after washing with different concentrations of $AgNO_3$: (a) 0.05, (b) 0.25, (c) 0.50, (d) 2.5, (e) 5.0 mmol. Peaks for Ag nanoparticles can be indexed according to their face centered cubic structure.

laponite disappeared, as shown in Figure 3(d) and (e), suggesting that laponite is exfoliated during freeze-drying. Ag-laponite nanocomposites are redispersed in water. Figure 4(a) shows a TEM micrograph of the exfoliated Ag-laponite nanocomposites, in which some of laponite layers appeared as dark stripes (Figure S1) and uniformly distributed. The shape and particle sizes of Ag nanoparticles are round, about 10-30 nm, implying that external faces of laponite are covered with Ag nanoparticles. To understand thermal behaviour

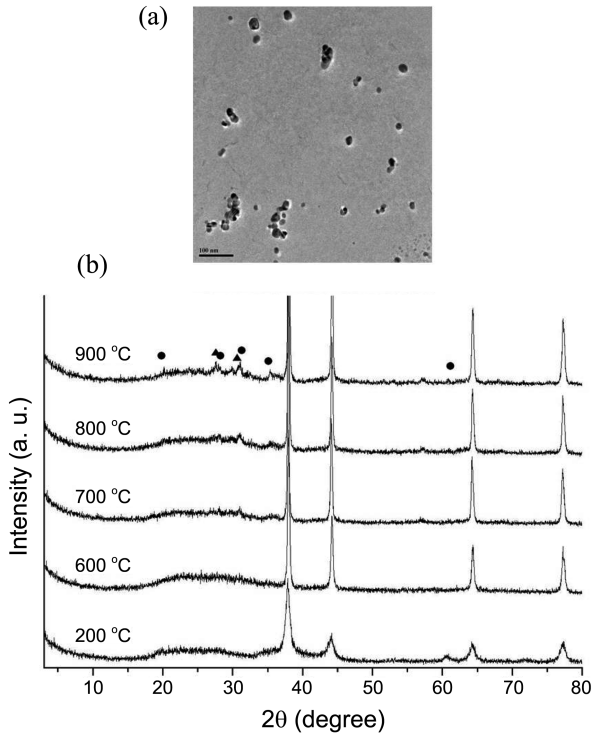

Figure 4. (a) TEM micrograph and (b) XRD patterns of exfoliated Ag-laponite nanocomposite after washing prepared in concentrations of $AgNO_3$: 2.5 mmol. The scale bar represents 100 nm. ● and ▲ represent orthoenstatite and protoenstatite, respectively.

of exfoliated Ag-laponite nanocomposites the sample was heated to various temperatures for 4 h in air as shown in Figure 4(b). The major new peaks started to appear at 700 °C and were attributed to the formation of enstatite polymorphs ($MgSiO_3$, JCPDS 19-0768 (orthoenstatite), 11-0273 (proto-enstatite)).[16] The XRD patterns of laponite decomposition for the thermally treated samples were consistent with those published for Eu^{3+} or Er^{3+} intercalated laponite powder,[17,18] confirming the presence of laponites. The nanosilver particle diameter calculated increases with the increase of temperature from 15 nm at 200 °C to 33 nm at 900 °C as shown in Figure 4(b). This study shows that there is a critical mole ratio (negative charge of laponite to $AgNO_3$ =1) for restacking of laponite in ordered face to face. In low content of silver ions, residual sodium ions diffused into the water would relocate between plate-like laponites to give stacked face to face in ordered tactoids. On the other hand in high content of silver ions a small amount of residual sodium ions are present and densly populated laponites adsorbed Ag nanoparticles with large size would interfere restacking of laponite in ordered fashion during a freeze-drying.

Experimental

Analytically pure $AgNO_3$ (Sigma-Aldrich, 99+%), $NaBH_4$ (Aldrich, 99%), NaOH (Daejung, 98%), and redistilled deionized water were used for all sample preparations. Laponite RD (Rockwood) was used without further purification and was considered as an anionic material with a negative charge (cationic exchange capacity) of about 50 mmol/100 g. Laponite RD (1.00 g, 0.50 mmol of negative charge) in 1000 mL water was set at pH 10 using NaOH (1 M, 5.5 mL) to avoid degradation.[19] The solution was vigorously stirred for 12 h using a mechanical stirrer and filtered through 0.45 μm pore size Millipore filters. Excess $NaBH_4$ (9.55 mg, 0.25 mmol) was added into the laponite solution and stirred for 5-10 more minutes. Separately, analytically pure $AgNO_3$ (8.58 mg, 0.05 mmol) in 100 mL water was prepared and Ag colloids in laponite sol were generated by slowly dropping silver nitrate solution in water into the laponite solution containing $NaBH_4$. The same procedure was conducted for the preparation of other concentrations of colloidal Ag nanoparticles. Ag-laponite nanocomposites were obtained with a freeze-drying process using a Samwon deep freezer (SFDSM24L). Ag-laponite nanocomposites were washed with distilled water three times and dried at room temperature. The morphology and size of the resulting products were analyzed by a transmission electron microscope (TEM; JEOL JEM-3010) operating at 300 kV. The absorption spectra of the nanoparticles were recorded on a UV2201 Shimadzu UV-vis spectrophotometer using optical quartz cells. The solid state characterization of nanoparticles in laponite was done by XRD (Rigaku, Ultima IV).

Acknowledgments. The present research was conducted under the research fund of Dankook University in 2013.

References

1. Alivisatos, A. P. *Nat. Biotechnol*. **2004**, *22*, 47.
2. Narayanan, R.; El-Sayed, M. A. *J. Phys. Chem. B* **2005**, *109*, 12663.
3. Valden, M.; Lai, X.; Goodman, D. W. *Science* **1998**, *281*, 1647.
4. Dimitrijevic, N. M.; Bartels, D. M.; Jonah, C. D.; Takahashi, K.; Rajh, T. *J. Phys. Chem. B* **2001**, *105*, 954.
5. Van Hyning, D. L,; Zukoski, C. F. *Langmuir* **1998**, *14*, 7034.
6. Liu, J.; Lee, J.-B.; Kim, D.-H.; Kim, Y. *Colloids Surf. A* **2007**, *302*, 276.
7. Fowden, L.; Barrer, R. M.; Tinker, P. B. *Clay Minerals: Their Structure, Behaviour and Use*; The Royal Society: London, 1984.
8. Shameli, K.; Ahmad, M. B.; Yunus, W. Z. W.; Ibrahim, N. A.; Darroudi, M. *Int. J. Nanomed.* **2010**, *5*, 743.
9. Patakfalvi, R.; Oszkó, A.; Dékány, I. *Colloids Surf. A* **2003**, *220*, 45.
10. Ayyappan, S.; Subbanna, G. N.; Gopalan, R. S.; Rao, C. N. R. *Solid State Ionics* **1996**, *84*, 271.
11. Hata, H.; Kobayashi, Y.; Salama, M.; Mallouk, T. E. *Chem. Mater.* **2007**, 1*9*, 6588.
12. Belova, V.; Möhwald, H.; Shchukin, D. G. *Langmuir* **2008**, *24*, 9747.
13. Liz-Marzań, L. M. *Langmuir* **2006**, *22*, 32.
14. Patterson A. L. *Phys. Rev.* **1939**, *56*, 978.
15. Yui, T.; Yoshida, H.; Tachibana, H.; Tryk, D. A.; Inoue, H. *Langmuir* **2002**, *18*, 891.
16. Green, J. M.; MacKenzie, K. J. D.; Sharp, J. H. *Clays and Clay Minerals* **1970**, *18*, 339.
17. Tronto, J.; Ribeiro, S. J. L.; Valim , J. B.; Gonçalves, R. R. *Mat. Chem. & Phys*. **2009**, *113*, 71.
18. Lee, H. N.; Kim, Y. *Bull. Korean Chem. Soc*. **2011**, *32*, 1273.
19. Thompson, D. W.; Butterworth, J. T. *J. Colloid. Interface Sci.* **1992**, *151*, 236.